Increasing the active surface in random sparse 2D arrays

Oscar Martínez[1], Carlos J. Martín[1], Alberto Octavio[2], Gregorio Godoy[3], Francisco Montero de Espinosa[2], Luis Gómez-Ullate[1]

1 Instituto de Automática Industrial (CSIC). Ctra Campo Real Km 0,200 (La Poveda) Arganda del Rey 28500 (Spain), oscarm@iai.csic.es

2 Instituto de Acústica (CSIC). C/Serrano, 144. Madrid. 28006 (Spain)

3 E.U.P. Linares, Universidad de Jaen, C/Alfonso X el Sabio, 28, 23700 Linares (Spain)

Abstract: The design process of a two-dimensional transducer arrays prototype for NDT air-coupling inspection is described. The manufacture process for the presented prototype, based on multiuser micro-electro-mechanical process (MUMPS), impose technical restrictions (like the size of membranes or the die size) that should be considered with the usual 2D apertures design drawbacks.

The development of full 2D squared matrix arrays suitable to generate high quality volumetric images is limited by the large number of elements needed. To avoid this inconvenience, several random sparse array design techniques have been proposed to reduce the number of active elements, maintaining good enough image quality. But unfortunately due to the high element impedance, as a consequence of its small size, and to the area reduction resulting from the thinning process, the image contrast is highly reduced.

In this paper we propose to increase the array active surface in random sparse arrays by enlarging the elements size up to λxλ, although we hold a λ/2xλ/2 element distribution grid. This strategy allows to increase the radiated energy and to reduce the element impedance, avoiding at the same time grating lobes formation. In the paper, we study theoretically the field properties of these arrays and, moreover, we make a comparison of the proposed solution with λxλ elements and the conventional arrays whose elements are kept under λ/2xλ/2.

Keywords: Ultrasonic imaging, 2D array, sparse bin-arrays, MUMPs.

A. Introduction

In some ultrasonic Non-Destructive Evaluation (NDE) applications there is an increasing interest in substituting liquid-coupling techniques by air-coupling, although these applications, due to absorption phenomena, are limited to low frequencies. Transducers based on MEMs technology can be employed in this application field. MEMs devices not only can be more efficient than piezoelectric transducers, furthermore this technology can facilitate the fabrication of complex apertures such as 2D arrays.

Due to the low frequencies needed, the use of multiuser MEMs process (MUMPs) can be justified, as it is simple and cost effective manufacture process. The MUMPs membranes are positioned in a die, grouped by the interconnections to compose the array elements. Unfortunately the membrane obtained by this technology (2μm tick) limits significantly the cell sensibility and consequently the element sensibility. To increase element efficiency several strategies around the cell configuration have been studied[1], but it is clear that the number of cells that compose is determinant to achieve this objective. This condition has special impact in the development of 2D array, where the element size is limited to λ/2 to avoid grating lobe formation.

One objective of this paper is to study these restrictions and propose solutions to design an air-coupling 2D array (fc=850KHz; diameter, D=40λ; λ=450μm) based on MUMPs technology. Now to the common 2D array design problems (high number of elements, N = 6400; difficult interconnection to pads [2]) we have to add those due to the MUMPs technology :

- The membrane size: which is around λ/3, limiting the element sensibility.

- The die size (10x10mm): which limits the array size and the number of elements pads.

To reduce the number of active elements several random sparse array design techniques have been described [3], unfortunately tied to this process there is a reduction of the image contrast, consequence to the emitting and reception area reduction. However the thinning strategy produce a lot of free space in the array surface, in this paper we propose use it to increase the element size (the number of membranes that compose the element) improving the emitting and reception area and the element sensibility.

Figure 1 presents three different element configurations 1x1 membranes (λ/3xλ/3), 2x2 membranes (λ2/3xλ2/3) and 3x3 membranes (λxλ); ANSY simulations have shown that the acoustic pressure is increased proportionally to the number of membranes. But the array response is modulated by the element diffraction pattern, so the element size is limited to λxλ to avoid reduce the array capability to steer the main lobe.

In the other hand, the die size is limited to 10x10mm (D=20λ) which is too small to compose larger arrays. So to cope with this inconvenience the array is divided in 4

different quadrants (4 die) to be assembled in the manufacture process. To reduce the cost, only one die/quadrant is designed, swapping it to compose a symmetric array. Furthermore the number of elements pads that can be used is limited, for the proposed solution only 64 pads per die are available so the array is limited to a 256 elements.

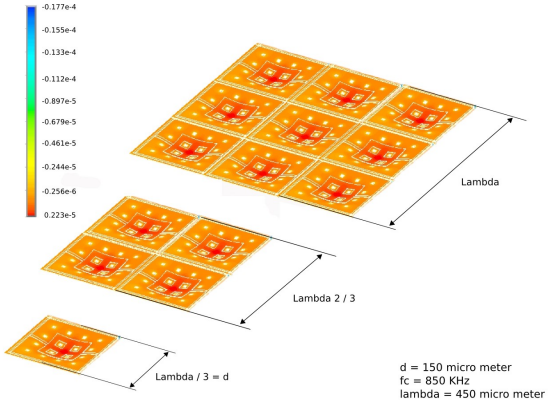

Fig.1. Three different element: 1x1 membranes (λ/3xλ/3), 2x2 membranes (λ2/3xλ2/3) and 3x3 membranes (λxλ)

In the rest of the paper the advantages and the inconveniences of these solutions will be examined and compared with a no restricted model. Matlab simulation models, based on pulse-echo response, have been developed:

- Array Factor [4]: Narrow Band
  - Point source response
- Spatial impulse response [5]: Wide Band
  - Point source response
  - Real size element response.

All the results presented are based on pulse-echo response using the same aperture in emission and reception with no apodization.

B. Array design

Increasing the element size introduces a restriction in the sparse element distribution that limits the design models that can be employed. In our case we have restricted our study to binned array.

To construct a binned array, the array (2D squared matrix arrays D=40λ) is divided into equal-sized bins; then one random position, in the λ/2 grid, is chosen per each bin, introducing in it a λxλ element that can restrict the possible locations in other bins. After that, a circular shape (R=20λ) is applied introducing another reduction of π/4 in the number of elements.

To construct the symmetric array, from the binned array the 1st quadrant is chosen (x>50μm, y>50μm due to a safe area), replied four times and swapped to complete the array (Figure 2).

We have studied both configuration with 3 different bin size (3x3, 4x4 and 5x5 elements), to evaluate the possible loss of quality in symmetric binned array respect to its original binned array. Each bin configuration has been analyzed with the Array Factor (1000 cases per each configuration). Results about number of elements and side lobes level (SL) are presented in tables 1 and 2.

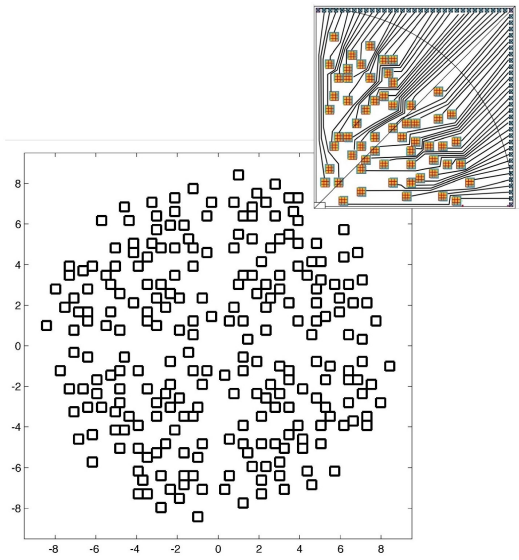

Fig.2. The symmetric binned array configuration implemented. A detail of 1st quadrant is presented.

Table 1. Side lobes statistical analysis.

Bin	Sym. B. Array		Binned Array	
	Mean	Min	Mean	Min
3x3	-28.48	-36	-29.4	-36.3
4x4	-27.04	-32.4	-30.0	-33
5x5	-23.6	-28	-26.22	-30

Table 2. Three best cases for each configuration.

Bin	Sym. B. Array		Binned Array	
	N.elem	Min SL	N. elem	Min SL
3x3	456	-35.3	490	-35.3
	460	-35.8	491	-36.3
	468	-36	495	-35.5
4x4	252	-31.5	268	-33
	264	-31.4	270	-33
	268	-32.4	274	-33
5x5	160	-28	174	-30
	164	-28	176	-30
	180	-28	180	-29

Although mean values are better for binned arrays, both apertures achieves similar values for the best solutions. So, in order to design the aperture no significant quality differences are found between both configurations, mainly when the bin size is small. It is possible to employ optimization methods to find the best

solution; but not all solutions are viable, interconnection routing should be considered to chose the most convenient configuration.

C. Array analysis

Figure 2 shows the implemented configuration. A 4x4 bin was applied to reduce the number of elements and several solution were examined to chose a viable aperture. Each die has 61 elements and 3 ground pads, then the array is composed by 244 elements. A detailed of the 1st quadrant where the interconnections wires are also presented.

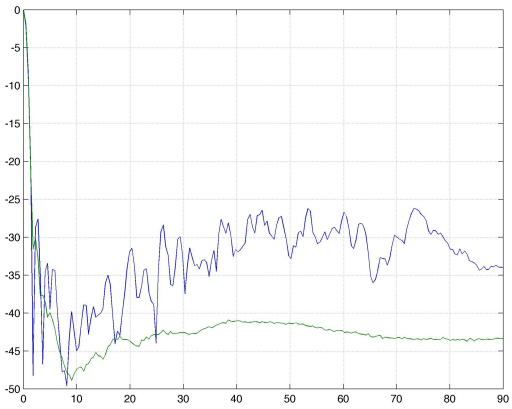

Fig.3. Maximum SL in elevation, Narrow band (blue line) and Wide Band (green line). Point source model.

In figure 3, the maximum SL measured with the Array Factor is -27dB, which is around the mean value obtained for a 4x4 bin. In spite of that it provides a good element distribution for the interconnection routing (at this stage of the research the main objective is just to evaluate the viability of this technology). Evaluating the wide band (BW=50%) response with the point source configuration and the spatial impulse response the maximum SL level is around -42dB.

In order to evaluate the consequence of using bigger elements, the spatial impulse model with the real size element was used to study different focusing conditions (R=80mm, ψ=0º, θ=0º, 5º, 10º, 15º, 20º, 25º and 30º) with both element sizes (apA λxλ and apB λ/2xλ/2). Results are shown in figure 4, where: the lateral profile (a.1 and b.1); the semi sphere (R=80mm) focusing at R = 80mm, ψ=0º, θ=30º (a.2, b.2); and the region (R=20:200mm, θ=-60º:60º, ψ=0º) focusing at R=80mm, ψ=0º, θ=30º (a.3, b.3) are presented.

The first significant observation in 4.a.1 and 4.b.1 is the higher decrease of the energy in the main beam with the elevation steering angle in the apA (-6dB, θ=30º) compared with apB (-2dB, θ=30º). Nevertheless there are no significant differences in the side lobe regions, furthermore lobes in high elevation regions are lower for apA than for apB.

In the figures 4.x.2 and 4.x.3 results are normalized to the maximum of the apA in order to remark the differences between both configurations.

- Both array present similar lobe structure, but all apB acoustic field structure is around -18dB under the apA.

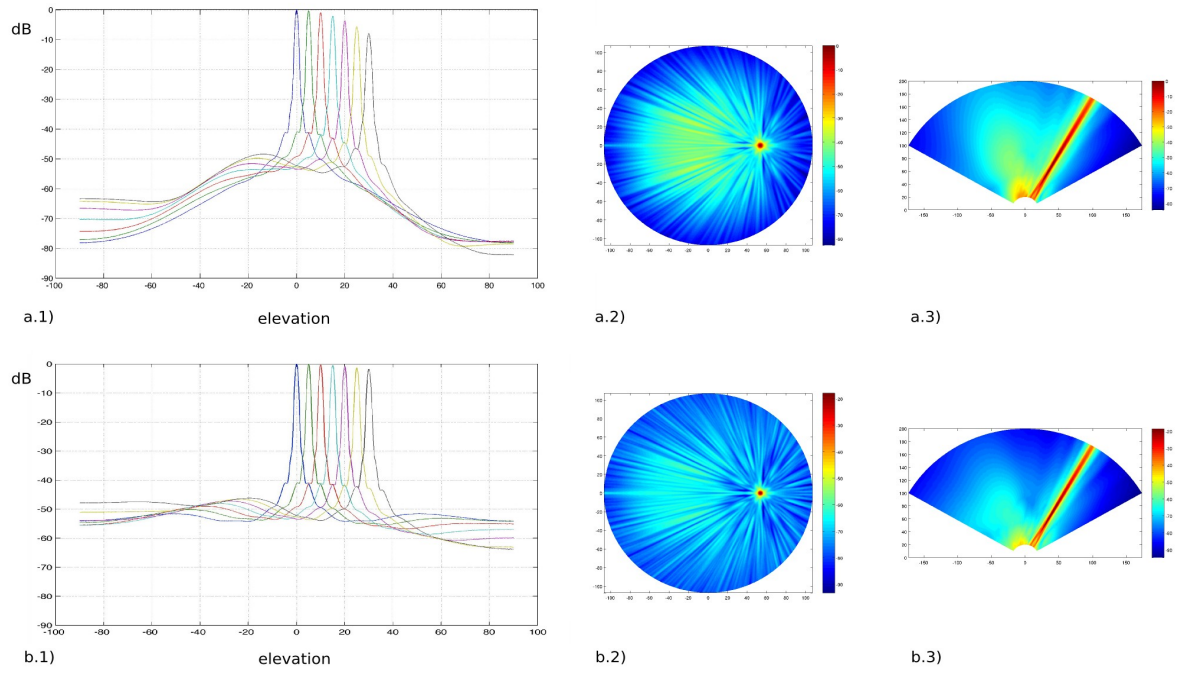

Fig.4. Acoustic pressure field computed with spatial impulse response (real elements size). Top aperture apA, bottom aperture apB. (a.1,b.1) lateral profile (R = 80mm, ψ=0º, θ=0º,5º,10º,15º,20º,25º and 30º) ; (a.2,b.2) the semi sphere (R=80mm) focusing at R=80mm, ψ=0º, θ=30º (a.2,b.2); and (a.3,b.3) region (R=20:200m, θ=-60º:60º, ψ=0º) focusing at R = 80mm, ψ=0º, θ=30º (a.3,b.3).

- The Main Lobe is well formed in both apertures, but it is slightly sharper in apB.
- The mean SL level of the apA is similar to apB level, but the highest apA SL are only around 3dB higher than the apB SL.
- In near field (before the focus) SL level is high (R<50mm) but after that point the energy is spread and SL level is under a convenient level, in apB this effect is located in a nearer region (R<25mm).

To find the reasons of these differences we have to analyze the figure 5. This figure represents the maximum ML (wide band) at each elevation angle (ψ=0º) in the focusing plane, it can be considered the lateral profile of the element diffraction pattern.

This figure shows:

- The difference in the MB pressure between both apertures, in θ=0º, apB is -22dB under apA, in θ=30º the difference is reduced to -18dB.
- It can be considered that there is a limit in the steering capabilities of apA aperture. It seems that more than θ=30º has a significant cost in dynamic range for the apA (under 40dB).
- This profile modules also the side lobe structure in elevation explaining the SL apA increase with the steering angle.

Results show that, although there are limits to the steering operation, it is possible to increase the energy radiated producing a behavior similar to apB. The limits in the steering region depends on the application requisites.

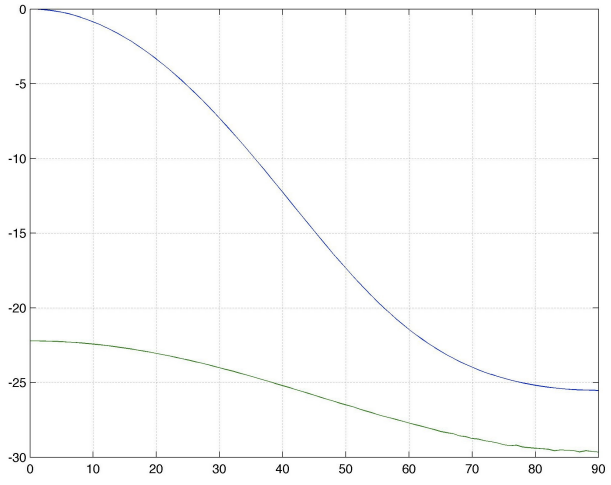

Fig.5. The maximum ML (wide band) at each elevation angle ψ=0, in the focusing plane for both configurations.

D. Array prototype

Figure 6 shows the developed prototype, details about elements layout and the interconnection with the pads are also shown. At that moment we have just received the prototype and it has not been tested yet, as soon as possible

E. Conclusions

1. A portotype of MMUPS air couplig 2D array for NDT applications has been developed with 244 elements

2. Restictions of MMUPS technology to design large 2D sparse arrays have been described and solved

3. Composing the array with 4 equal quadrants has derived in the development of a Symmetric Bin-arrays, allowing to reduce the manufacturing costs, the design process and the element interconnection routing.

4. Increasing the element size 1x1 membrane to 3x3 membranes (from λ/3xλ/3 to λxλ)

- Element sensibility is increased.

- The energy radiated is increased by 9.

5. Unfortunately the steering capabilities of the array are reduced to θ = 30º.

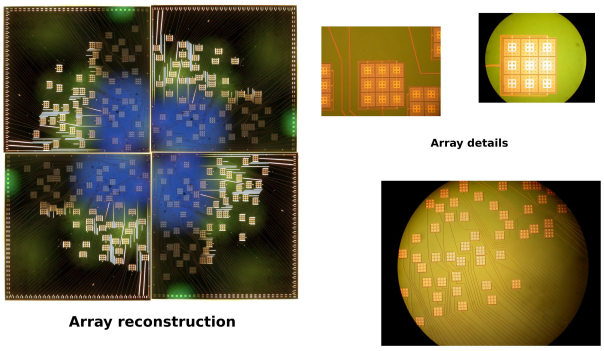

Fig.6. Photo pictures of 1st quadrant apA prototype, details of the elements connections are also presented. A reconstruction of the apA is presented.

F. Aknowledgements

The financial support of Spanish Ministry of Education and Science (project DPI2004-06756-C03-03 and DPI2004-06470) is acknowledged.

G. Literature

[1] A.O. Manzanares et al. Design of air coupled ultrasonic transducers based on MUMPs. 5th Instenational workshop on MUT. Munich 2006.

[2] B.D. Steinberg, Principles of Aperture and Array System. New York: Wiley 19719

[3] A. Austeng and S. Holm. Sparse 2-D Arrays for 3-D Phased Array Imaging—Design Methods. ieee UFFC 49(8) 2002. pp. 1073-1086

[4] C.A. Balanis, Antenna theory. New York: Wiley 1982.

[5] B. Piwakowski and K. Sbai A New Approach to Calculate the Field Radiated from Arbitrarily Structured Transducer Arrays. ieee UFFC 46(2). 1999. pp. 422-440.